Simulation of Tunnel Current in an Armchair Graphene Nanoribbon-Based p-n Diode for Undergraduate Physics Students

Rifky Syariati, Endi Suhendi, Fatimah A. Noor, Khairurrijal[1]

Physics of Electronic Material Research Division,
Faculty of Mathematics and Natural Sciences, Institut Teknologi Bandung
Jalan Ganesa 10, Bandung 40132, Indonesia
[1]krijal@fi.itb.ac.id

Abstract - Simulation of tunnel current flowing in a p-n diode made from armchair graphene nanoribbons (AGNRs) was built. The diode is composed of p-type and n-type AGNRs and bandgaps of the AGNRs are obtained by using a tight binding method. The bandgaps are required to describe a potential profile having a potential barrier of the diode. Transmittance of electrons tunneling through the potential barrier is then calculated by employing Airy wavefunctions. Gaussian quadrature method, which is a numerical approximation, is used to obtain tunnel current in the diode. All steps are visualized by using the graphical user interface of Matlab.

Index Terms - Armchair graphene nanoribbon, tunnel current, tight binding, Airy-wave function, gaussian quadrature, diode.

1. Introduction

Recently, learning the properties of graphene seems to be quite common for physics students both in the experiment and simulation. It is not strange because graphene has made breakthrough as the pioneer of 2-D materials [1]. Beside of that, for device applications, graphene has electronic properties which are believed as a base for high speed devices since it has high thermal stability, high electron and hole mobilities, and massless electron [2].

Graphene in nanometer scale known as graphene nanoribbon (GNR) has two types: armchair GNR (AGNR) and zigzag GNR (ZGNR). They are in different characteristics; AGNR is known as a semiconductor while ZGNR as a conductor [2-5]. The semiconductor properties of AGNR can therefore be explored in designing and realizing electronic devices such as p-n junction diodes and field-effect transistors. Unfortunately, there is no simulator to visualize tunnel current in a p-n junction diode based on AGNRs for undergraduate physics students.

In this paper, we describe the simple tight binding method to obtain the bandgap of AGNR. After that, the bandgap of AGNR is employed to find an energy band diagram of AGNR-based p-n junction diode and its potential barrier. Once the potential barrier is known, the transmittance of electrons tunneling through the potential barrier is then calculated by employing Airy wavefunctions. Gaussian quadrature method, which is a numerical approximation, is used to obtain tunnel current in the diode. Matlab with its graphical user interface is used to calculate all steps and visualize the potential barrier and tunnel current of the diode.

2. Physical Basis of Simulator

The first step in calculating tunnel current in the p-n junction diode is to obtain the band gap of AGNR. This band gap can be obtained by using tight binding method, in which a geometry structure and atomic positions in a material lattice are very important. As shown in Fig.1, the atomic positions of AGNR are written as:

$$m_1 = ae_y, \tag{1}$$

$$m_2 = \frac{\sqrt{3}}{2}a(e_x - \frac{1}{\sqrt{3}}e_y), \tag{2}$$

$$m_3 = \frac{\sqrt{3}}{2}a(e_x - \frac{1}{\sqrt{3}}e_y), \tag{3}$$

where a is the distance between two carbon atoms.

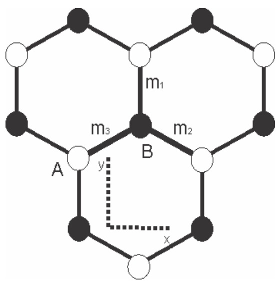

Figure 1. A schematic view of lattice structure and atomic positions of AGNR

In AGNR, the Hamiltonian and the energy dispersion relation are defined by [2].

$$H = \begin{pmatrix} E_o & tf(k) \\ tf^*(k) & E_o \end{pmatrix} \tag{4}$$

$$E(k) = E_o \pm t\left|f(k)\right|. \tag{5}$$

Here, E_o is the initial energy of electron, t is the overlapping parameter with the magnitude of 2.76 eV, and $f(k)$ is the geometry factor. The geometry factor when the valence and conduction band in the low states is described by [2].

$$f\left(K+p\right)\approx\sum_{m_1}e^{-iKm_1}\left(1-ipm_1\right). \tag{6}$$

where $K=\frac{4\pi}{3\sqrt{3}a}e_x$ and p is a slight shift of the K point. Substituting the atomic positions (Eqs. (1) to (3)) into Eqs. (4) to (6), the energy dispersion relation is written as [3, 5].

$$E=\pm\frac{3at}{2}\sqrt{p_x^2+p_y^2}. \tag{7}$$

Here, the symbol ± indicates the valence and conduction bands, respectively. p_x and p_y are the wave number in the x- and y-axis, respectively, and it is assumed that the initial energy of electron is zero. The bandgap E_G can be found from the relation $E_G=E_C–E_V$. Because the length of AGNR is restricted in the x-axis and infinite in the y-axis, the wave number in the x-axis is defined by [2].

$$p_x=\frac{\pi n}{W_{ac}+\sqrt{3}a}+\frac{4\pi}{3\sqrt{3}a} \tag{8}$$

where W_{ac} is the width of AGNR.

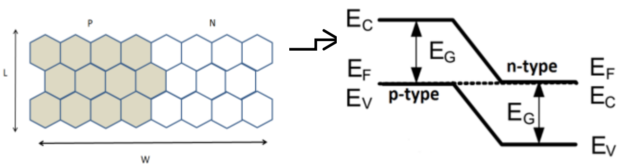

(a)

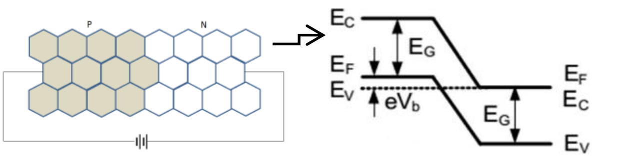

(b)

Figure 2. (a) An energy band diagram of a p-n junction diode in thermal equilibrium, and (b) when the reserve-bias voltage is applied to a p-n junction.

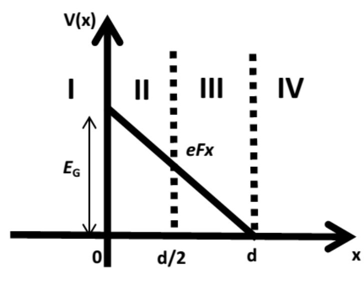

Figure 3. A triangular potential barrier occurs in the depletion region when a small bias voltage is applied to the p-n junction diode.

After the band gap is obtained, the next step is to obtain an energy band diagram of the p-n junction. Figure 2.(a) shows that the p-n junction is in the thermal equilibrium. In this condition, it is assumed that the valence band of the p-type is equal to the conduction band of the n-type of AGNR. After the reverse bias was applied to the p-n junction diode, which is depicted in Fig.2.(b), the valence band of the p-type increases, so that its electrons have a probability to tunnel the depletion region, which is formed in the p-n junction region, to the conduction band of the n-type. This condition is known as Zenertunnel. The depletion region is therefore represented by a triangular potential barrier as given in Fig. 3 [6,7].

In order to obtain electron transmittance when tunneling the triangular potential barrier, the triangular potential is divided into four regions. Because there is a potential slope in regions II and III (see Fig. 3), the Airy wavefunction will be used in those regions. The wavefunction for each region is defined by:

$$\psi_I\left(x\right)=A\exp\left(ik_1x\right)+B\exp\left(-ik_1x\right), x<0\ , \tag{9}$$

$$\psi_{II}\left(x\right)=C\,Ai\left(\zeta\left(x\right)\right)+D\,Bi\left(\zeta\left(x\right)\right), 0\le x\le\frac{d}{2}, \tag{10}$$

$$\psi_{III}\left(x\right)=E\,Ai\left(\xi\left(x\right)\right)+F\,Bi\left(\xi\left(x\right)\right), \frac{d}{2}\le x\le d, \tag{11}$$

$$\psi_{IV}\left(x\right)=G\exp\left(ik_2x\right), x>d\quad , \tag{12}$$

where A, B, C, D, E, F, and G are constant, Ai and Bi are Airy function, $d=E_G/\mathrm{eF}$ is the depletion region thickness and F is the electric field in the depletion region. In Eq.(9) the wave number in the region I is written as:

$$k_1=\sqrt{\frac{2M_1E}{\hbar^2}}, \tag{13}$$

where M_1 is the electron effective mass in p-junction, E is electron energy and $\hbar$ is reduced Planck constant. In the regions II and III the Airy function is expressed by:

$$\zeta\left(x\right)=\left(\frac{2M_1eF}{\hbar^2}\right)^{\frac{1}{3}}\left(\frac{E_G-E}{eF}-x\right), \tag{14}$$

$$\xi\left(x\right)=\left(\frac{2M_2eF}{\hbar^2}\right)^{\frac{1}{3}}\left(\frac{E_G-E}{eF}-x\right), \tag{15}$$

where M_2 is electron effective mass in n-junction, E_G is the band gap and F is the applied electric field. And then for the region IV, the wave number is illustrated by:

$$k_2=\sqrt{\frac{2M_2E}{\hbar^2}} \tag{16}$$

Applying the boundary conditions between two regions with formulation $\psi_i=\psi_{i+1}$ and $\frac{\partial\psi_i}{\partial x}=\frac{\partial\psi_{i+1}}{\partial x}$. Here $I\le i\le III$, the wave function becomes:

$$\begin{bmatrix}1 & 1\\ ik_1 & -ik_1\end{bmatrix}\begin{bmatrix}A\\ B\end{bmatrix}=\begin{bmatrix}Ai\left(\zeta\left(0\right)\right) & Bi\left(\zeta\left(0\right)\right)\\ w_1Ai'\left(\zeta\left(0\right)\right) & w_1Bi'\left(\zeta\left(0\right)\right)\end{bmatrix}\begin{bmatrix}C\\ D\end{bmatrix},\quad x=0, \tag{17}$$

$$\begin{bmatrix} Ai\left(\zeta\left(\frac{d}{2}\right)\right) & Bi\left(\zeta\left(\frac{d}{2}\right)\right) \\ w_1 Ai'\left(\zeta\left(\frac{d}{2}\right)\right) & w_1 Bi'\left(\zeta\left(\frac{d}{2}\right)\right) \end{bmatrix} \begin{bmatrix} C \\ D \end{bmatrix} = \begin{bmatrix} Ai\left(\xi\left(\frac{d}{2}\right)\right) & Bi\left(\xi\left(\frac{d}{2}\right)\right) \\ w_2 Ai'\left(\xi\left(\frac{d}{2}\right)\right) & w_2 Bi'\left(\xi\left(\frac{d}{2}\right)\right) \end{bmatrix} \begin{bmatrix} E \\ F \end{bmatrix}, \quad x = \frac{d}{2}, \tag{18}$$

$$\begin{bmatrix} Ai(\xi(d)) & Bi(\xi(d)) \\ w_2 Ai'(\xi(d)) & w_2 Bi'(\xi(d)) \end{bmatrix} \begin{bmatrix} E \\ F \end{bmatrix} = e^{ik_2 d} \begin{bmatrix} G \\ ik_2 G \end{bmatrix}, \quad x = d. \tag{19}$$

where $w_1 = \left(\frac{2M_1 eF}{\hbar^2}\right)^{\frac{1}{3}}$ and $w_2 = \left(\frac{2M_2 eF}{\hbar^2}\right)^{\frac{1}{3}}$. From the equations (17), (18), and (19), using matrix operation, the transmittance is written as

$$T = \frac{k_2}{k_1}\left(\left(\frac{G}{A}\right)^* \left(\frac{G}{A}\right)\right). \tag{20}$$

The electron transmittance is then used to calculate the tunnel current which is given by:

$$I = \frac{2g_v e}{h} \int_0^{eV_b} \left[f_v(E) - f_c(E) \right] T dE \tag{21}$$

where $f_v(E) = 1/\left(1 + exp\left[\left(E - eV_b\right)/k_b T\right]\right)$ and $f_c(E) = 1/\left(1 + exp\left[E/k_b T\right]\right)$ are the Fermi-Dirac distributions in the valence and the conduction bands, respectively, k_b is Boltzmann constant, g_v is GNR degeneration which has a magnitude of 1, and $\hbar$ is the Planck constant. The tunnel current is calculated using Gaussian Quadrature method which can be generated in Matlab.

3. Results and Discussion

Figure 4 shows the triangular potential barrier which is influenced by the electric field of 1 MV/cm and the AGNR width of 10 nm. The height and slope length of the potential can be altered by those parameters. The electric field has a role in extending and shortening the slope of the potential barrier. On the other hand, the AGNR width can change the height of the potential barrier.

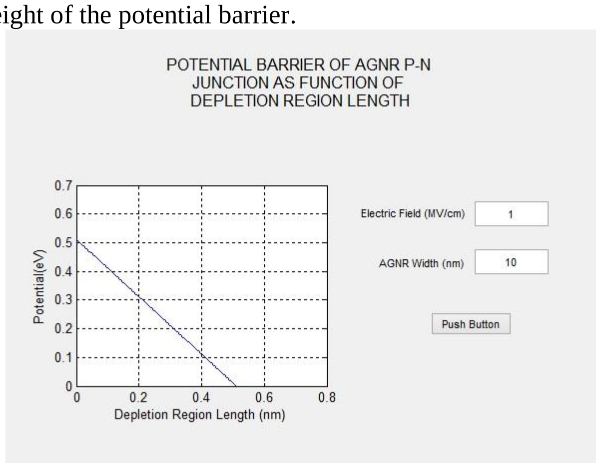

Figure 4. Simulation of potential barrier in AGNR p-n junction with parameters F=1 MV/cm and W_{ac}= 10 nm.

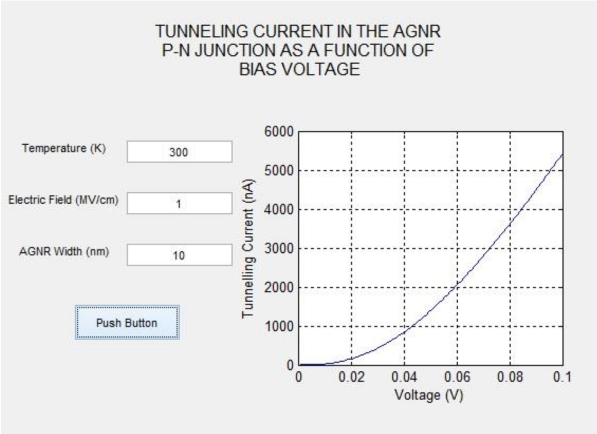

Figure 5. Simulation of tunnel current in AGNR p-n junction with parameters T=300 K, F=1 MV/cm, and W_{ac}= 10 nm.

Figure 5 gives simulation of tunnel current obtained by using the following parameters: temperature, electric field, and AGNR width are 300 K, 1 MV/cm, and 10 nm, respectively. It is found that the tunnel current increases with increasing the voltage bias. The tunnel current will be different if the temperature, electric field, and AGNR width are changed. In Refs.[6,7], it was shown that if the temperature and the AGNR width are increased and the electric field is decreased, the tunnel current will decrease. On the contrary, if the temperature and the AGNR width are low and small, respectively, and the electric field is high, then the tunnel current will be high. This condition occurs because temperature, electric field, and AGNR width influence the height of the potential barrier in the depletion region so that the electron penetration into the triangular potential barrier is tuned by those parameters.

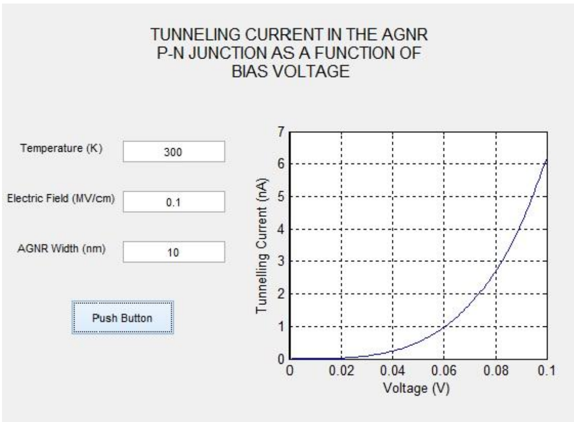

Figure 6. Simulation of tunnel current in AGNR p-n junction with parameters$T$=300 K, F=0.1 MV/cm, and W_{ac}= 10 nm.

Figure 6 illustrates the tunnel current as a function of bias voltage with the electric field of 0.1 MV/cm and the AGNR width of 10 nm at a temperature of 300 K. By comparing Fig. 6 to Fig. 5, it is shown that by decreasing the electric field, the tunnel current will also decrease. This condition occurs because the decrease of the electric field will extend the slope length of potential barrier so that the probability of electron to tunnel the potential barrier is reduced.

The tunnel current with the temperature of 300 K, the electric field of 1 MV/cm, and the AGNR width of 3 nm is demonstrated in Fig.7. It was found that the tunnel current decreases when the AGNR width is reduced. This happens because reducing the AGNR width will have the same effect with elevating the height of the potential barrier. If the height of the potential barrier is higher than before, electrons require more energy to tunnel the potential barrier.

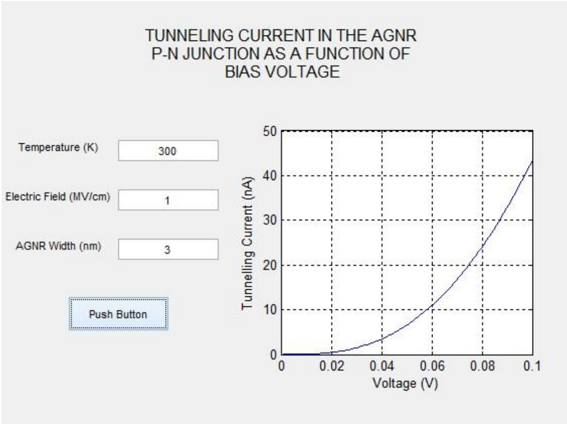

Figure 7. Simulation of tunnel current in AGNR p-n junction with parameters T=300 K, F=1 MV/cm, and W_{ac}= 3 nm.

4. Conclusions

We have studied step by step how to obtain the tunnel current in an AGNR-based p-n junction diode. In the first step, we gave how to find the bandgap using the tight binding method. After that, we applied the bandgap to the p-n junction diode to obtain a potential barrier and electron transmittance though the potential barrier was calculated by using Airy wavefunctions. In the last step, we employed Gaussian quadrature method to obtain tunnel current in the p-n junction diode. All steps are visualized by using the graphical user interface of Matlab.

Acknowledgments

This work was financially supported by "Hibah Desentralisasi", "Riset & Inovasi KK", and "Hibah Kompetensi" Research Grants in the fiscal year 2013-2014.

References

[1] A. K. Geim and K. S. Novoselov, "The rise of graphene," *Nat. Mater.* vol.6, pp. 183-191, March 2007.

[2] C. Neto, F. Guinea, R. Peres, S. Novoselov, and K. Geim, "The electronic properties of graphene," *Rev. Mod. Phys*. vol. 81. p.109, Jan. 2009.

[3] H. Zheng, Z. F. Wang, T. Luo, O. W. Shi, and J. Chen, "Analytical study of electronic structure in armchair graphene nanoribbons," *Phys. Rev. B*, vol.75, p. 165414, April 2007.

[4] J. Fernandez-Rossier, J. J. Palacios, and L. Brey, "Electronic structure of gated graphene and graphene ribbons, " *Phys. Rev. B*, vol.75, p. 205441, May 2007.

[5] Y. W. Son, M. L. Cohen, and S. G. Louie, "Energy gaps in graphene nanoribbons, " *Phys. Rev. Lett*., vol. 97, p. 216803, 2006.

[6] D. Jena, T. Fang, Q. Zhang, and H. Xing, "Zener tunneling in semiconducting nanotube and graphene nanoribbon p-n junctions," *Appl. Phys. Lett*., vol 93, p.112106, Sept. 2008.

[7] W. Yansen, M. Abdullah, and Khairurrijal, "Application of Airy Function approach to model electron tunneling in graphene nanoribbon-based p-n junction diodes," *Jurnal Nanosains & Nanoteknologi*, vol.3, no.1, pp. 18-21, Feb. 2010.